

Evolution of the gas mass fraction in galaxy clusters

Irina Dvorkin^{1*}, Yoel Rephaeli^{1,2}

¹*School of Physics and Astronomy, Tel Aviv University, Tel Aviv, 69978, Israel*

²*Center for Astrophysics and Space Sciences, University of California, San Diego, La Jolla, CA 92093-0424*

6 December 2024

ABSTRACT

The mass fraction of hot gas in clusters is a basic quantity whose level and dependence on the cluster mass and redshift are intimately linked to all cluster X-ray and SZ measures. Modeling the evolution of the gas fraction is clearly a necessary ingredient in the description of the hierarchical growth of clusters through mergers of subclumps and mass accretion on the one hand, and the dispersal of gas from the cluster galaxies by tidal interactions, galactic winds, and ram pressure stripping on the other hand. A reasonably complete description of this evolution can only be given by very detailed hydrodynamical simulations, which are, however, resource-intensive, and difficult to implement in the mapping of parameter space. A much more practical approach is the use of semi-analytic modeling that can be easily implemented to explore a wide range of parameters. We present first results from a simple model that describes the build up of the gas mass fraction in clusters by following the overall impact of the above processes during the merger and accretion history of each cluster in the ensemble. Acceptable ranges for model parameters are deduced through comparison with results of X-ray observations. Basic implications of our work for modeling cluster statistical properties, and the use of these properties in joint cosmological data analyses, are discussed.

Key words: galaxies: clusters: general - intracuster medium

1 INTRODUCTION

Hot intracluster (IC) gas is an important cluster component that determines X-ray emission quantities and the nature and properties of the Sunyaev-Zel'dovich (SZ) effect. Cluster X-ray and SZ surveys provide a broad basis for exploring key statistical properties of the population, such as the mass function, and are valuable cosmological probes of, e.g., the equation of state of dark energy, the amplitude of primordial density fluctuations and the neutrino mass (e.g. Vikhlinin et al. 2009; Mantz et al. 2010b; Lueker et al. 2010; Shimon et al. 2012; Planck Collaboration et al. 2013b). However, both X-ray emission and the SZ signal of a cluster of a given mass are very sensitive to the hot gas mass fraction f_{gas} , which is not known precisely and - in principle - can depend on the mass and redshift of the cluster. While it is expected that f_{gas} should be close to the cosmic value Ω_b/Ω_m by virtue of the large size of clusters, some of the baryons are locked in cluster galaxies, and therefore do not contribute to the respective observable. Therefore, it is of interest to model

the fraction of hot, X-ray emitting gas in galaxy clusters, particularly at high redshifts.

Observational effort to determine f_{gas} is motivated also by the basic need to study the evolution of the total baryon fraction in groups and clusters, which has contributions also from galaxies and IC light (e.g. White et al. 1993; Mohr, Mathiesen & Evrard 1999; Ettori 2003; Lin, Mohr & Stanford 2003; Gonzalez, Zaritsky & Zabludoff 2007; Giodini et al. 2009; McCarthy, Bower & Balogh 2007). In several of these works the reported baryon fraction is smaller than the expected value, particularly in low-mass systems. The observed trend is an increase of the fraction of hot gas with total system mass, approximately following $f_{gas} \propto M^{0.1-0.2}$, and a decrease of the stellar fraction as $f_s \propto M^{-(0.4-0.6)}$ (Lin, Mohr & Stanford 2003; Gonzalez, Zaritsky & Zabludoff 2007; Sun et al. 2009). A possible interpretation of the mass dependence of f_{gas} is that gas is expelled from low-mass systems due to non-gravitational processes, such as feedback from active galactic nuclei (AGN) (Scannapieco & Oh 2004). In this scenario more massive systems retain a larger fraction of their gas due to their deeper potential wells.

* E-mail: irina@wise.tau.ac.il

Another important piece of evidence is the observed metallicity of IC gas, with a mean value of $\simeq 1/3$ solar (e.g. Finoguenov, David & Ponman 2000; De Grandi & Molendi 2001; Vikhlinin et al. 2005; Baldi et al. 2012), and with a decreasing radial profile. Since metals are produced only in stars, it follows that a large fraction of IC gas was ejected from galaxies. Indeed, numerical simulations (e.g. Kapferer et al. 2007; Arieli, Rephaeli & Norman 2010) show that ejection of metals from galaxies can account for the observed metallicity. This interpretation is further strengthened by the observed evolution of the galaxies in clusters (the Butcher-Oemler effect), namely that the fraction of blue galaxies is higher at higher redshifts (Butcher & Oemler 1978); note though that the significance of this effect is uncertain due to difficulties in disentangling the influence of the chosen galaxy sample and secular evolution (Raichoor & Andreon 2012). Moreover, spirals found in clusters tend to be redder (Hughes & Cortese 2009), HI deficient as compared to similar galaxies in the field (Solanes et al. 2001), and typically have truncated gaseous discs (Koopmann, Haynes & Catinella 2006). These observations suggest that galaxies lost most or all of their gas since they first fell into the cluster, either due to encounters with other galaxies, or as a result of ram-pressure stripping, as discussed below. This led to the quenching of star formation and the subsequent change of color and morphology.

The baryonic fraction in clusters, particularly the fraction of hot gas, was extensively studied using cosmological hydrodynamical simulations (e.g. Ettori et al. 2006; Borgani et al. 2006; Young et al. 2011; Planelles et al. 2013). While the observed mass dependence of f_{gas} is generally well reproduced by these simulations, the stellar mass fraction is typically larger than observed, which may be due to the fact that the (correct) gas mass fraction is attained by an overestimated star formation rate. In general, numerical simulations are computationally expensive, which complicates the modeling of the interplay between galactic and large-scale phenomena.

An alternative semi-analytic model, proposed by Bode, Ostriker & Vikhlinin (2009) (see also Ostriker, Bode & Babul 2005) is based on the assumption that f_{gas} in all halos was initially equal to the cosmic baryon fraction, and that it decreased due to the processes of star formation and ejection of gas out of the halo by SN-and-AGN-driven winds. This model is calibrated to X-ray observations of nearby clusters, and so successfully reproduces the local cluster population.

In this paper we take a different approach: motivated by the observed metallicity and galaxy (color) evolution, we assume that a large fraction of the IC gas was ejected from galaxies. In this picture f_{gas} increases with mass because larger systems typically form later through mergers of smaller systems, and therefore their galaxies had more time to eject their gas. As we show in this paper, our model directly links galactic processes (which can be described by small-scale numerical simulations) with various cluster-scale observables.

Several processes may be responsible for mass ejection from cluster galaxies. When a galaxy traverses the higher density inner region of a cluster, ram-pressure effectively removes an appreciable fraction of its interstellar gas (Gunn & Gott 1972). The details of this

process depend on the IC gas density profile, galactic gas density profile, and the trajectory of the galaxy (Abadi, Moore & Bower 1999; Vollmer et al. 2001; Hester 2006; Tecce et al. 2010), all of which are difficult to model, but it is clear that ram pressure can remove large quantities of gas from the galaxy on relatively short timescales (e.g. Quilis, Moore & Bower 2000). Observational evidence for this process comes from the tails behind several cluster galaxies seen in HI, H α and X-rays, interpreted as removal of galactic ISM (e.g. Sun, Donahue & Voit 2007; Ebeling, Stephenson & Edge 2014). In addition, tidal interactions between field galaxies are known to affect the distribution of gas and stars within the galaxies, and may be as important in cluster galaxies, especially in dense cluster cores (Merritt 1983; Moore et al. 1999; Gnedin 2003). Tidal interactions truncate the dark matter density profile of subhalos orbiting inside a massive cluster, which leads to more concentrated profiles of subhalos relative to field halos (Bullock et al. 2001; Limousin et al. 2009). The transformation of spirals into S0 galaxies in clusters and the existence of 'passive spirals' (which are morphologically identical to normal spirals but lack star formation activity) may be related to these environmental effects (e.g. Bekki, Couch & Shioya 2002; Just et al. 2010).

Another major feedback process that affects galaxy evolution is galactic winds. SN-driven winds are particularly important at high redshifts, when the star formation rate (SFR) is high (e.g. Pettini et al. 2001). A sufficiently fast wind deposits metal-enriched material into IC space. As the SFR drops at low redshifts, metal enrichment effects of galactic winds become sub-dominant to ram pressure and tidal interactions. Therefore we focus on these environmental processes which are closely related to the mass accretion history of the cluster.

In this paper we build a phenomenological model of gas ejection in the context of the hierarchical assembly of clusters and explore the range of possible models and their consequences for X-ray and SZ cluster surveys. We adopt the following cosmological parameters: $H_0 = 67.11$ km/s/Mpc, $\Omega_m = 0.3175$, $\Omega_\Lambda = 0.6825$, $\sigma_8 = 0.8344$, and $n_s = 0.9624$ (Planck Collaboration et al. 2013a). In Section 2 we briefly describe our model of cluster evolution, which is based on an extended merger tree code that follows the evolution of halos that consist of dark matter and baryons. Gas ejection from galaxies and the build-up of f_{gas} is discussed in Section 3. Our results are presented in Section 4 and discussed in Section 5.

2 CLUSTER MERGER-TREE EVOLUTION

The efficiency of interstellar (IS) gas removal by tidal interactions and ram pressure depends on the depth of the cluster gravitational potential. This occurs continuously through a series of interaction and merger events during the dynamical evolution of a galaxy in a growing cluster. We follow the evolutionary history of IC gas by considering the overall impact of the above galactic processes in a statistical description based on a merger tree code.

In the Λ CDM framework structure forms hierarchically, starting with relatively low mass halos that grow successively through mergers and accretion. The merger

history of a given cluster can be described by a *merger tree*, which essentially is a list of the masses of the merging halos and the redshifts at which these mergers occurred. The mass assembly history of a cluster affects its density profile (Wechsler et al. 2002) and causes an intrinsic scatter in all the mass-observable relations. In previous works (Dvorkin & Rephaeli 2011; Dvorkin, Rephaeli & Shimon 2012) we studied how the hierarchical formation of galaxy clusters affects their X-ray and SZ properties; here we extend our merger-tree approach to include an approximate description of some basic galaxy-scale processes.

In order to describe the evolution of galaxy clusters we build merger trees of dark matter halos using the GALFORM algorithm (Parkinson, Cole & Helly 2008) which is based on the excursion set formalism (Lacey & Cole 1993). For a cluster with a given mass and at a given observation redshift each merger tree represents a possible formation history, and a sufficiently large number of merger trees can provide a statistical description of the population. The advantage of using this kind of semi-analytic modeling is our ability to produce a large number of clusters (equivalent to simulating a very large volume of the Universe) by employing an efficient algorithm that can be readily applied to explore the parameter space of the model.

Instead of using a constant redshift step for the output of the merger tree, we save the information on all the progenitors with masses $M > M_{res}$, where M_{res} is the mass resolution limit. The merger trees of Parkinson, Cole & Helly (2008) are calibrated to match the Sheth-Tormen mass function (Sheth & Tormen 1999), which we use throughout this paper for consistency. The original DM-only merger-tree code was extended to include also IC gas, whose density and temperature profiles are determined from basic considerations (essentially, energy conservation and hydrostatic equilibrium). Further details on the merger tree algorithm and its implementation for clusters of galaxies can be found in Parkinson, Cole & Helly (2008) and Dvorkin & Rephaeli (2011).

We follow the evolution of all halos in a tree (i.e. all the progenitors of the given cluster) with (total) masses $M > M_{res} = 10^{11} M_{\odot} h^{-1}$ that existed below redshift $z = 2$. The number of galaxies in a halo scales linearly with its mass,

$$N_{gal}(M) = N_{gal,0} \left(\frac{M}{10^{11} M_{\odot} h^{-1}} \right) \quad (1)$$

where $N_{gal,0}$ is a model parameter. At high enough redshift large structures are rare; therefore, their member galaxies are expected to resemble low-redshift galaxies in the field, i.e. they should be relatively massive blue disks. We assign an initial mass for these galaxies $M_{gal,i} = 10^{11} M_{\odot} h^{-1}$, a value that decreases by the various mass loss processes.

An alternative method of describing the galaxy population would be to explicitly account for subhalos and follow them as distinct systems even after they merge with the main halo. This kind of approach (i.e. Yoo et al. 2007) necessitates modeling the trajectory of each galaxy inside the main halo, taking into account dynamical friction, encounters with other subhalos, and the impact of subsequent mergers of the main halo with other systems. While this kind of approach provides a more accurate description of cluster growth, it might be difficult to pinpoint the key physical

processes that influence the evolution of IC gas. Therefore, we chose to assign all the galaxies the same (fiducial) initial mass, which is reduced at later stages of evolution as described below. We note that our model effectively averages over all possible galaxy masses and trajectories, as well as the merger impact parameters.

The diffuse inter-halo gas mass fraction (which could originate from early galactic winds) is f_{diff} at the initial time, so that $M_{gas,i} = f_{diff} \cdot (M - M_{gal,i} N_{gal})$, whereas galaxies are assumed to have the cosmic baryon fraction $f_c = \Omega_b / \Omega_m$. Clearly, baryon ejection processes from galaxies affect the stellar component, the disk, and the warm gas in the galactic halo.

3 MODELING IC ENVIRONMENTAL PROCESSES

When galaxies fall onto larger structures, they experience tidal interactions with the host halo and other subhalos. The strength of these interactions depends on the host halo mass, or on the local density of galaxies, which is ultimately also determined by the host mass. Tidal interactions affect the dark matter, as well as IS gas, so that cluster galaxies are expected to have truncated dark matter profiles (Limousin et al. 2009). This truncation enhances the effect of ram pressure stripping by making the galaxy potential wells effectively shallower.

Numerical simulations show that the time scale of gas removal from galaxies through ram pressure is relatively short (Quilis, Moore & Bower 2000), and that the fraction of gas-depleted galaxies is a strong function of host halo mass (Hester 2006; Tecce et al. 2010). Thus, although the ram pressure experienced by a galaxy moving in a cluster varies between a maximal value attained at the cluster center and a minimal value in the outskirts (Brüggen & De Lucia 2008), most loosely bound gas is likely to be ejected upon first passage through the center. Further stripping occurs when the galaxy is in a deeper potential well, i.e. after a merger with a larger halo. This episodic mass loss and the connection between ram pressure stripping and the merging history of the cluster is demonstrated by the numerical simulations of Kapferer et al. (2007). On the other hand, the model by Hester (2006) shows that for a galaxy of a given mass there exists a limiting cluster mass for which ram pressure is strong enough to remove almost all of the gas even in the innermost regions of the galaxy, while for smaller cluster masses almost none of the gas is removed.

Motivated by these findings, we assume that after each merger event a fraction

$$f_m = f_{m,0} \left(\frac{M}{10^{14} M_{\odot} h^{-1}} \right)^{\alpha} \quad (2)$$

of the total galactic mass is removed, of which f_c is in baryons:

$$\Delta M_{gas} = f_m f_c N_{gal} M_{gal}. \quad (3)$$

Accordingly, the mass of a typical galaxy residing in this halo is reduced to account for the mass loss

$$M_{gal} \rightarrow M_{gal} \cdot (1 - f_m). \quad (4)$$

The parameter α describes the steepness of the dependence

of gas removal on cluster mass; for large values of α there will be a very pronounced transition from insignificant environmental effects to very rapid mass ejection from the galaxy, whereas for small values of α the ejection process is more gradual.

We approximate the virialization phase of gas removed from galaxies by assuming that it is immediately heated to the virial temperature of the host halo. Thus, the hot gas content of a halo immediately after a merger event is

$$M_{gas}(M) = M_{gas}(M_1) + M_{gas}(M_2) + \Delta M_{gas} + \Delta M_{gas,diff} \quad (5)$$

where M_1, M_2 are the two merging halos (typically the host halo and a smaller halo), ΔM_{gas} is calculated as in eq. (3), and $\Delta M_{gas,diff}$ is the gas contained in diffuse matter that falls onto the halo.

These equations are employed following each merger event, so that the gas content of the cluster increases as the cluster evolves and the mean mass of cluster galaxies is decreased.

4 RESULTS

4.1 IC gas fraction and metallicity

We ran 1000 tree realizations for each halo mass with mass resolution of $M_{res} = 10^{11} M_\odot h^{-1}$ and up to $z = 2$. We considered all merger events between halos above this resolution mass. Mergers with smaller halos were considered as part of the smooth accretion process, as described above.

Fig. 1 shows the hot gas mass fraction in clusters in the mass range $10^{13} M_\odot h^{-1} - 10^{15} M_\odot h^{-1}$ as predicted by our model, and compared with data from several X-ray studies. Parameters of the fiducial model, shown in black, are: $N_{gal,0} = 0.5, f_{diff} = 0.11, f_{m,0} = 0.01, \alpha = 1.84$. We compare our model with X-ray observations of groups and clusters (points with error-bars) and find good agreement. These results suggest that the mass dependence of f_{gas} can be largely explained by environmental processes. To obtain an estimate for the range of parameter values that are consistent with the data, we show by the blue lines in Fig. 1 the approximate region that brackets the range of values of the three datasets. These upper and lower lines correspond to the parameters $N_{gal,0} = 0.7, f_{diff} = 0.14, f_{m,0} = 0.045, \alpha = 0.39$ and $N_{gal,0} = 0.3, f_{diff} = 0.0725, f_{m,0} = 0.01, \alpha = 1.55$, respectively. Note though that the comparison with observations has only a limited value due to substantial modeling uncertainty, mainly in the cluster mass determination from X-ray observables.

An analytical fit to the fiducial model is

$$f_{gas} = c \left(1 + e^{-[\log_{10}(M/M_\odot) - a]/b} \right)^{-1} + d \quad (6)$$

with $a = 14.291, b = 0.135, c = 0.051, d = 0.072$, while the corresponding parameters for the upper and lower uncertainty limits (blue lines in Fig. 1) are $a = 13.953, b = 0.295, c = 0.071, d = 0.078$ and $a = 14.317, b = 0.148, c = 0.029, d = 0.059$, respectively. The fit demonstrates the transition to efficient mass stripping, which occurs around $M = 10^a M_\odot$.

No explicit redshift dependence is deduced from our results, in line with the usual assumptions (e.g. Allen et al.

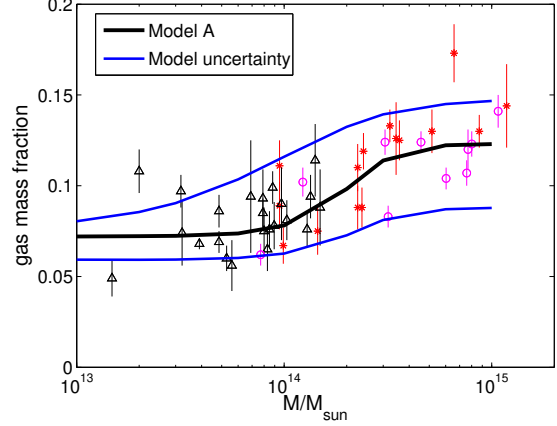


Figure 1. Gas mass fraction vs. cluster mass for the fiducial model (black line; parameter values are specified in the text) with model uncertainty range bracketed by the blue lines. X-ray measurements inside M_{500} from Gonzalez et al. (2013, red stars), Vikhlinin et al. (2006, magenta circles) and Sun et al. (2009, black triangles).

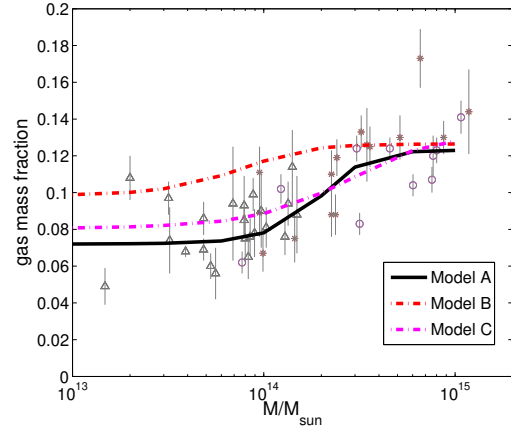


Figure 2. Gas mass fraction vs. cluster mass for 3 representative models: Model A (also shown on Fig. 1): $N_{gal,0} = 0.5, f_{diff} = 0.12, f_{m,0} = 0.01, \alpha = 1.75$, Model B: $N_{gal,0} = 0.3, f_{diff} = 0.12, f_{m,0} = 0.01, \alpha = 1$ and Model C: $N_{gal,0} = 0.5, f_{diff} = 0.12, f_{m,0} = 0.01, \alpha = 0.7$. Points with error bars show the X-ray measurements, specified in the caption of Figure 1.

2008). The reason for this is that in our model the efficiency of gas removal from cluster galaxies depends on the mass of the host halo, but not explicitly on the redshift at which galaxy infall occurs. Note though that the dependence on mass clearly introduces implicit redshift dependence through the strong mass dependence of the probability distribution function of cluster formation times (e.g. Sadeh & Rephaeli 2008).

Fig. 2 shows the results of our model for three representative sets of parameters: Model A (the fiducial model shown on Fig. 1), Model B: $N_{gal,0} = 0.3, f_{diff} = 0.12, f_{m,0} = 0.01, \alpha = 1$ and Model C: $N_{gal,0} = 0.5, f_{diff} = 0.12, f_{m,0} = 0.01, \alpha = 0.7$. In all three models the gas mass fraction increases with mass by $\sim 20-50\%$ from groups to rich clusters, respectively. This trend is largely determined by the follow-

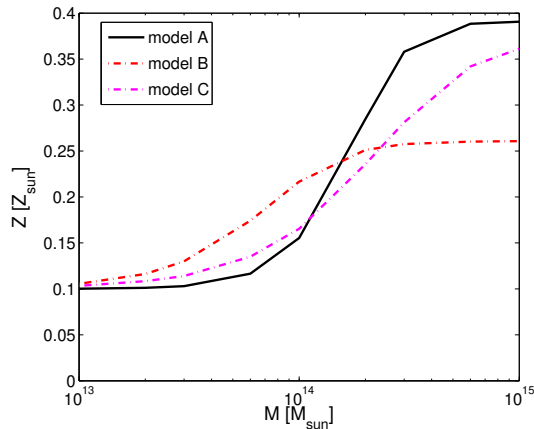


Figure 3. Metal abundance (in units of the solar value) for models A, B and C for which the corresponding f_{gas} is shown in Fig. 2.

ing model parameters: $N_{gal,0}$, which is related to the amount of gas initially locked inside galaxies, and f_{diff} , which is the gas fraction in diffuse matter. The latter parameter is expected to be high, but lower than the universal value f_c since baryons are more clustered than dark matter. The parameters $f_{m,0}$ and α quantify the environmental processes that galaxies undergo as the cluster is assembled and affect the transition from the low f_{gas} level in groups to a high level in rich clusters. In particular, the steepness of this transition is determined by the value of α (see eq. 2).

While a more complete and quantitative description of gas ejection processes requires a high spatial resolution hydrodynamical simulation that can follow individual galaxy trajectories, our simple treatment seems to provide an adequate basis for comparison with the data. The good agreement of the predicted mass dependence of f_{gas} with the observations clearly indicates that *on average* cluster environmental processes may be described by a few universal model parameters. Interestingly, the observed f_{gas} exhibits large scatter, which may be linked to the scatter in these unresolved parameters. Quantifying the connection between the varying galactic trajectories, composition, IC gas density profile, values of the merger impact parameter, and the scatter in our effective model parameters, is an important future goal (which is clearly beyond the scope of our simplified treatment).

IC gas metallicity provides additional insight on the evolution of the gas mass fraction. Gas that was removed from galaxies obviously has higher metal abundance than the inter-cluster gas, which we refer to as IGM. However, the metallicity Z_i of the IGM that accretes into the cluster could be higher than that of primordial gas, since it could have already been enriched by galactic outflows (Werner et al. 2013). On the other hand, the metallicity of galactic gas, Z_{gal} depends on the stellar mass and probably also on the environment of the galaxy (Peng & Maiolino 2014). Since these parameters depend on processes that occurred before $z = 2$, long before the cluster had assembled, we do not attempt to model them here, instead we adopt effective constant values for both Z_i and Z_{gal} .

Fig. 3 shows the metallicity of the IC gas for vari-

ous cluster masses with $Z_i = 0.1$ and $Z_{gal} = 0.8$. It can be seen that although all three models produce similar $f_{gas}(M)$ they can be further distinguished by their very different mass-metallicity relations (which, however, depend on the assumed ratio of Z_i/Z_{gal}). The differences between the selected models are mostly evident for the most massive clusters, but also for $M \lesssim 10^{14} M_\odot$ which roughly corresponds to the halo mass for which environmental effects become important. Interestingly, there seems to be some observational evidence (Rasmussen & Ponman 2009; Sasaki, Matsushita & Sato 2014) for an increase of the mean metal abundance with IC gas temperature, and hence with system mass. Further investigation of the chemical composition of IC gas in groups and clusters will help constrain our model and provide more information on the processes of gas enrichment.

4.2 X-ray luminosity function

Modeling $f_{gas}(M)$ is particularly important in view of the ongoing and upcoming X-ray and SZ cluster surveys, whose main objectives are the study of cluster properties and the use of clusters as precise cosmological probes. These surveys, when jointly analyzed together with complementary cosmological probes (such as CMB anisotropies and baryonic acoustic oscillations) can shed light on the physics of galaxy clusters and the nature of mass-observable relations. The latter are shaped by cosmological structure formation, as well as small-scale physics. Therefore, the magnitude of f_{gas} and its M & z dependence may effectively serve as a means of studying the main physical processes affecting galaxies in dense environments, provided the cosmological parameters are constrained fairly well by complementary probes. In particular, the f_{gas} models proposed here can be used to link X-ray observables to galactic processes in clusters.

First we calculate the scaling relation between the bolometric X-ray luminosity and the emission weighted temperature inside R_{500} . In order to calculate the density and temperature profile we assume a polytropic model, so that the pressure and density are related by $P = P_0(\rho/\rho_0)^\Gamma$ with $\Gamma = 1.2$. Then the solution of the equation of hydrostatic equilibrium for a polytropic gas inside a potential well of a DM halo is (Ostriker, Bode & Babul 2005):

$$\rho(x) = \rho_0 \left[1 - \frac{B}{1+n} \left(1 - \frac{\ln(1+x)}{x} \right) \right]^n, \quad (7)$$

where $n = (\Gamma - 1)^{-1}$, $B = 4\pi G \rho_s r_s^2 \mu m_p / k_B T_0$, μm_p is the mean molecular weight and $r_s = R/c$ is the scale radius of the cluster, and c is the concentration parameter. The temperature profile is given by:

$$T(x) = T_0 \left[1 - \frac{B}{1+n} \left(1 - \frac{\ln(1+x)}{x} \right) \right]. \quad (8)$$

We take the halo concentration parameters from our merger-tree model, which describes the dark matter density profile as a function of the formation history of the cluster (Dvorkin & Rephaeli 2011; Dvorkin, Rephaeli & Shimon 2012).

Figure 4 shows the bolometric luminosity L_X vs. emission weighted temperature for model clusters at $z = 0$ compared with low-redshift observations. Our model uncertainty, derived from the scatter in f_{gas} brackets the observa-

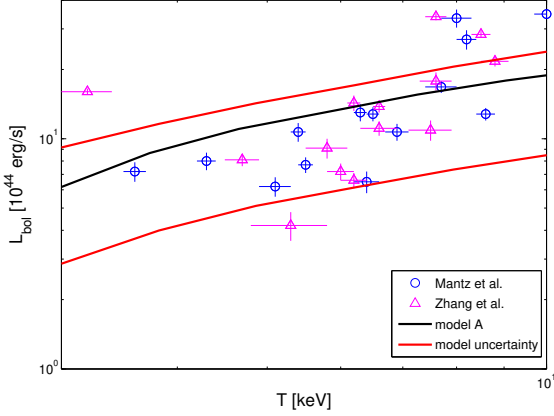


Figure 4. $L_X - T$ relation computed using the fiducial f_{gas} model (black line) and model uncertainty region (red lines) compared with X-ray measurements from Zhang et al. (2008) and Mantz et al. (2010a)

tions, as expected. The observed scatter in the X-ray scaling relations might be due to different dynamical state of some of the clusters (i.e. they could be out of equilibrium due to a recent merger event), as well as variations in f_{gas} .

Additional information is provided by the cluster luminosity function. Recently, Böhringer, Chon & Collins (2014) used the REFLEX II cluster survey to construct the X-ray luminosity function and to derive constraints on Ω_m and σ_8 . Future surveys will be able to extend this analysis to higher redshifts, probing the mass function and thermodynamical properties of these systems.

Figure 5 shows the expected luminosity function for redshifts up to $z = 0.5$ in the measured 0.1 – 2.4 keV spectral band, which corresponds to the energy range of ROSAT measurements. We used the Sheth-Tormen mass function for consistency with the merger tree algorithm we employ. In the future we plan to extend this work by calibrating the merger tree building code to more general mass functions, so as to carry out a more detailed comparison with results of hydrodynamical simulations.

4.3 SZ power spectrum

Recent findings by the *Planck* Collaboration (2013) indicate that there is ‘tension’ between the observed SZ power spectrum and cluster number counts and theoretical predictions based on primary CMB observations. One of the possible culprits is the gas mass fraction, which links the dark matter halo abundance, predicted by theory, to the observed SZ signal, which results from interaction of CMB photons and hot IC electrons. It is quite interesting, therefore, to check whether our range of f_{gas} models can alleviate the tension reported by *Planck*.

We compute the SZ power spectrum using the halo approximation (Komatsu & Seljak 2002):

$$C_\ell = s(\chi)^2 \int_0^{z_{max}} \frac{dV(z)}{dz} dz \int_{M_{min}}^{M_{max}} dM \frac{dn}{dM} |y_\ell(M, z)|^2 \quad (9)$$

where $s(\chi)$ is the spectral dependence of the SZ signal given

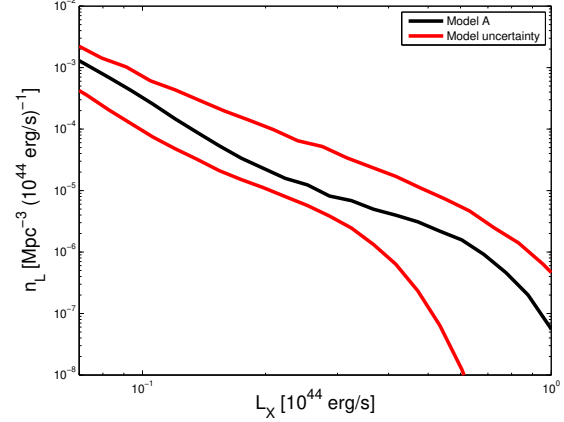


Figure 5. X-ray luminosity function computed using the fiducial f_{gas} model (black line) and model uncertainty region (red lines) for clusters in the range $z = 0 - 0.5$.

by:

$$s(\chi) = \chi \frac{e^\chi + 1}{e^\chi - 1} - 4, \quad (10)$$

$\chi = h\nu/k_B T_0$ is the dimensionless frequency, $V(z)$ is the comoving volume per steradian, and dn/dM is the mass function. The 2D Fourier transform of the projected Comptonization parameter is

$$y_\ell = \frac{4\pi r_s}{\ell_s^2} \int_0^c dx x^2 \frac{\sin(\ell x/\ell_s)}{\ell x/\ell_s} \zeta(x) \quad (11)$$

where $\ell_s = d_A(z)/r_s$, $d_A(z)$ is the angular diameter distance to the cluster, and $\zeta(x)$ is the gas (normalized) pressure

$$\zeta(x) = \frac{k_B \sigma_T}{m_e c^2} n_e(x) T_e(x). \quad (12)$$

Typical parameters are $z_{max} = 2$, $M_{min} = 10^{13} h^{-1} M_\odot$ and $M_{max} = 10^{16} h^{-1} M_\odot$. The concentration parameter is calculated as above, using our merger-tree model of cluster evolution. The temperature and density profiles are given by eq. (7)-(8).

The resulting thermal SZ power spectrum is shown in Fig. 6. Given the cosmological parameters deduced from primary CMB observations by *Planck* (adopted in this work) our fiducial model is in tension with *Planck* measurements of the SZ power spectrum. This result reflects the $\sim 2\sigma$ discrepancy between the values of σ_8 and Ω_m deduced from primary CMB vs. cluster number counts (Planck Collaboration et al. 2013b). We demonstrate the important implication of this discrepancy by the dashed black line in Fig. 6, calculated with our fiducial f_{gas} model and $\sigma_8 = 0.78$, which corresponds to the 2σ lower limit of the *Planck* primary CMB value. It is apparent, then, that the uncertainty in the value of σ_8 can largely explain the discrepancy with the deduced SZ power spectrum, even if other additional uncertainties in cluster parameters (such as the mass function and the gas equation of state) are ignored.

5 DISCUSSION

We developed a simple and efficient model that accurately describes the mass dependence of the hot gas mass fraction

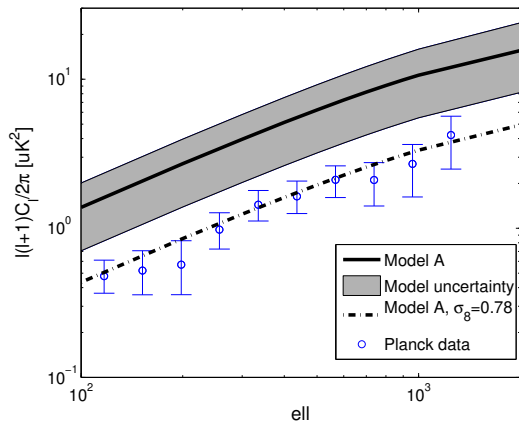


Figure 6. SZ power spectrum for the fiducial model (black line) and the model uncertainty region (grey stripe) that corresponds to the blue lines on Fig. 1. Also shown are measurements from *Planck* (blue circles), and the fiducial model with $\sigma_8 = 0.78$, which corresponds to the lower 2σ limit of the constraint from *Planck* (dashed black line).

in clusters. Our model links two important physical phenomena: the morphological transformation (and mass loss) of cluster galaxies under the influence of the dense cluster environment, and the evolution of the hot gas. Our results show that the possible relation between these processes can be understood in terms of a few parameters with intuitive physical interpretation: The amount of galaxies, the gas fraction of diffuse matter, and the efficiency of gas removal from galaxies which we modeled as a power-law in halo mass. At present, none of these parameters is known with high precision; detailed hydrodynamical simulations are needed in order to determine the properties of high-redshift galaxies and to better understand the IC processes that affect the evolution of their IS gas.

However, our model offers an alternative way to understand IC gas evolution through comparison with the observed f_{gas} and metallicity. While it is computationally challenging to develop and run hydrodynamical simulations of cosmological structure formation that also resolve structure and (relatively) small-scale galactic processes, such as ram pressure stripping, our approach provides a convenient framework for studying the important gas ejection processes. A general model can be derived by fitting $f_{gas}(M)$ measurements, as demonstrated above. This model predicts specific dependence of the efficiency of gas removal from galaxies, which can be tested against small-scale numerical simulations of ram pressure and tidal stripping, processes whose quantitative assessment does not require the full framework of a cosmological simulation. Such simulations can be run with different galactic masses and ambient IC gas densities to study how these parameters contribute to the scatter in $f_{m,0}$ and α that control gas removal efficiency in our model. Additional constraints can be provided by measurements of IC gas metallicity, as demonstrated in the previous section.

An important and timely application of our simple numerical approach is the prediction of the SZ power spectrum. We reproduce the $\sim 2\sigma$ discrepancy between the models based on cosmological parameters deduced from pri-

mary CMB observations, and the observationally deduced (by *Planck*) thermal SZ power spectrum. While the range of model parameters adopted here do not seem to resolve this discrepancy, the insight gained from our treatment can be useful in future studies of the SZ effect, which will allow better assessment of the uncertainties resulting from IC gas physics.

We plan to extend this work by implementing different mass functions and thereby providing much more accurate calculations of the cluster statistical measures. Another route of investigation is the introduction of cluster-to-cluster scatter in our model parameters and their scatter using the observables discussed above - $f_{gas}(M)$, metallicity, X-ray scaling relations and luminosity function, and SZ power spectrum - and providing a handle on the details of the environmental processes that mostly affect cluster galaxies. These results can be used as an input, or compared against, small-scale simulations of galaxies in an ambient gas environment, where the modeling of galactic structure and dynamics inside the cluster can be controlled.

ACKNOWLEDGMENTS

The authors wish to thank the GALFORM team for making the code publicly available. Work was partly supported by the James B. Ax Family Foundation.

REFERENCES

- Abadi M. G., Moore B., Bower R. G., 1999, MNRAS, 308, 947
- Allen S. W., Rapetti D. A., Schmidt R. W., Ebeling H., Morris R. G., Fabian A. C., 2008, MNRAS, 383, 879
- Arieli Y., Rephaeli Y., Norman M. L., 2010, ApJ, 716, 918
- Baldi A., Ettori S., Molendi S., Balestra I., Gastaldello F., Tozzi P., 2012, A&A, 537, A142
- Bekki K., Couch W. J., Shioya Y., 2002, ApJ, 577, 651
- Bode P., Ostriker J. P., Vikhlinin A., 2009, ApJ, 700, 989
- Böhringer H., Chon G., Collins C. A., 2014, ArXiv e-prints
- Borgani S. et al., 2006, MNRAS, 367, 1641
- Brüggen M., De Lucia G., 2008, MNRAS, 383, 1336
- Bullock J. S., Kolatt T. S., Sigad Y., Somerville R. S., Kravtsov A. V., Klypin A. A., Primack J. R., Dekel A., 2001, MNRAS, 321, 559
- Butcher H., Oemler, Jr. A., 1978, ApJ, 219, 18
- De Grandi S., Molendi S., 2001, ApJ, 551, 153
- Dvorkin I., Rephaeli Y., 2011, MNRAS, 412, 665
- Dvorkin I., Rephaeli Y., Shimon M., 2012, MNRAS, 421, 2648
- Ebeling H., Stephenson L. N., Edge A. C., 2014, ApJ, 781, L40
- Ettori S., 2003, MNRAS, 344, L13
- Ettori S., Dolag K., Borgani S., Murante G., 2006, MNRAS, 365, 1021
- Finoguenov A., David L. P., Ponman T. J., 2000, ApJ, 544, 188
- Giodini S. et al., 2009, ApJ, 703, 982
- Gnedin O. Y., 2003, ApJ, 582, 141

- Gonzalez A. H., Sivanandam S., Zabludoff A. I., Zaritsky D., 2013, *ApJ*, 778, 14
- Gonzalez A. H., Zaritsky D., Zabludoff A. I., 2007, *ApJ*, 666, 147
- Gunn J. E., Gott, III J. R., 1972, *ApJ*, 176, 1
- Hester J. A., 2006, *ApJ*, 647, 910
- Hughes T. M., Cortese L., 2009, *MNRAS*, 396, L41
- Just D. W., Zaritsky D., Sand D. J., Desai V., Rudnick G., 2010, *ApJ*, 711, 192
- Kapferer W. et al., 2007, *A&A*, 466, 813
- Komatsu E., Seljak U., 2002, *MNRAS*, 336, 1256
- Koopmann R. A., Haynes M. P., Catinella B., 2006, *AJ*, 131, 1716
- Lacey C., Cole S., 1993, *MNRAS*, 262, 627
- Limousin M., Sommer-Larsen J., Natarajan P., Milvang-Jensen B., 2009, *ApJ*, 696, 1771
- Lin Y.-T., Mohr J. J., Stanford S. A., 2003, *ApJ*, 591, 749
- Lueker M. et al., 2010, *ApJ*, 719, 1045
- Mantz A., Allen S. W., Ebeling H., Rapetti D., Drlica-Wagner A., 2010a, *MNRAS*, 406, 1773
- Mantz A., Allen S. W., Rapetti D., Ebeling H., 2010b, *MNRAS*, 406, 1759
- McCarthy I. G., Bower R. G., Balogh M. L., 2007, *MNRAS*, 377, 1457
- Merritt D., 1983, *ApJ*, 264, 24
- Mohr J. J., Mathiesen B., Evrard A. E., 1999, *ApJ*, 517, 627
- Moore B., Lake G., Quinn T., Stadel J., 1999, *MNRAS*, 304, 465
- Ostriker J. P., Bode P., Babul A., 2005, *ApJ*, 634, 964
- Parkinson H., Cole S., Helly J., 2008, *MNRAS*, 383, 557
- Peng Y.-j., Maiolino R., 2014, *MNRAS*, 438, 262
- Pettini M., Shapley A. E., Steidel C. C., Cuby J.-G., Dickinson M., Moorwood A. F. M., Adelberger K. L., Giavalisco M., 2001, *ApJ*, 554, 981
- Planck Collaboration et al., 2013a, *ArXiv e-prints*
- Planck Collaboration et al., 2013b, *ArXiv e-prints*
- Planelles S., Borgani S., Dolag K., Ettori S., Fabjan D., Murante G., Tornatore L., 2013, *MNRAS*
- Quilis V., Moore B., Bower R., 2000, *Science*, 288, 1617
- Raichoor A., Andreon S., 2012, *A&A*, 543, A19
- Rasmussen J., Ponman T. J., 2009, *MNRAS*, 399, 239
- Sadeh S., Rephaeli Y., 2008, *MNRAS*, 388, 1759
- Sasaki T., Matsushita K., Sato K., 2014, *ApJ*, 781, 36
- Scannapieco E., Oh S. P., 2004, *ApJ*, 608, 62
- Sheth R. K., Tormen G., 1999, *MNRAS*, 308, 119
- Shimon M., Rephaeli Y., Itzhaki N., Dvorkin I., Keating B. G., 2012, *MNRAS*, 427, 828
- Solanes J. M., Manrique A., García-Gómez C., González-Casado G., Giovanelli R., Haynes M. P., 2001, *ApJ*, 548, 97
- Sun M., Donahue M., Voit G. M., 2007, *ApJ*, 671, 190
- Sun M., Voit G. M., Donahue M., Jones C., Forman W., Vikhlinin A., 2009, *ApJ*, 693, 1142
- Tecce T. E., Cora S. A., Tissera P. B., Abadi M. G., Lagos C. D. P., 2010, *MNRAS*, 408, 2008
- Vikhlinin A., Kravtsov A., Forman W., Jones C., Markevitch M., Murray S. S., Van Speybroeck L., 2006, *ApJ*, 640, 691
- Vikhlinin A. et al., 2009, *ApJ*, 692, 1060
- Vikhlinin A., Markevitch M., Murray S. S., Jones C., Forman W., Van Speybroeck L., 2005, *ApJ*, 628, 655
- Vollmer B., Cayatte V., Balkowski C., Duschl W. J., 2001, *ApJ*, 561, 708
- Wechsler R. H., Bullock J. S., Primack J. R., Kravtsov A. V., Dekel A., 2002, *ApJ*, 568, 52
- Werner N., Urban O., Simionescu A., Allen S. W., 2013, *Nature*, 502, 656
- White S. D. M., Navarro J. F., Evrard A. E., Frenk C. S., 1993, *Nature*, 366, 429
- Yoo J., Miralda-Escudé J., Weinberg D. H., Zheng Z., Morgan C. W., 2007, *ApJ*, 667, 813
- Young O. E., Thomas P. A., Short C. J., Pearce F., 2011, *MNRAS*, 413, 691
- Zhang Y.-Y., Finoguenov A., Böhringer H., Kneib J.-P., Smith G. P., Kneissl R., Okabe N., Dahle H., 2008, *A&A*, 482, 451